

Molecular simulation of the thermophysical properties and phase behaviour of impure CO₂ relevant to CCS - Electronic Supplementary Information

Alexander J. Cresswell^a, Richard J. Wheatley^b, Richard D. Wilkinson^c, and
Richard S. Graham^a

^a *School of Mathematical Sciences, University of Nottingham, Nottingham NG7 2RD, UK.*

^b *School of Chemistry, University of Nottingham, Nottingham NG7 2RD, UK.*

^c *School of Mathematics and Statistics, University of Sheffield, Western Bank Sheffield,
S10 2TN UK.*

February 26, 2016

1 Force-field optimisation

We optimised the impurity force-field for CO₂+N₂, CO₂+O₂, CO₂+Ar and CO₂+H₂, in turn, using the simplex method as described in the text of the main article. The measurements used for fitting, along with the predictions of the initial and final force-fields are shown in figures 1-6. The evolution of the lowest error on the simplex with iteration number, for these optimisations is shown in figures 7- 9. The simplex optimisation was ended when the difference between error terms at different points on the simplex becomes of the same order as the statistical uncertainties of the simulations. At this point simplex had shrunk sufficiently that no further meaningful improvement in the agreement could be achieved. This typically required 10-20 iterations.

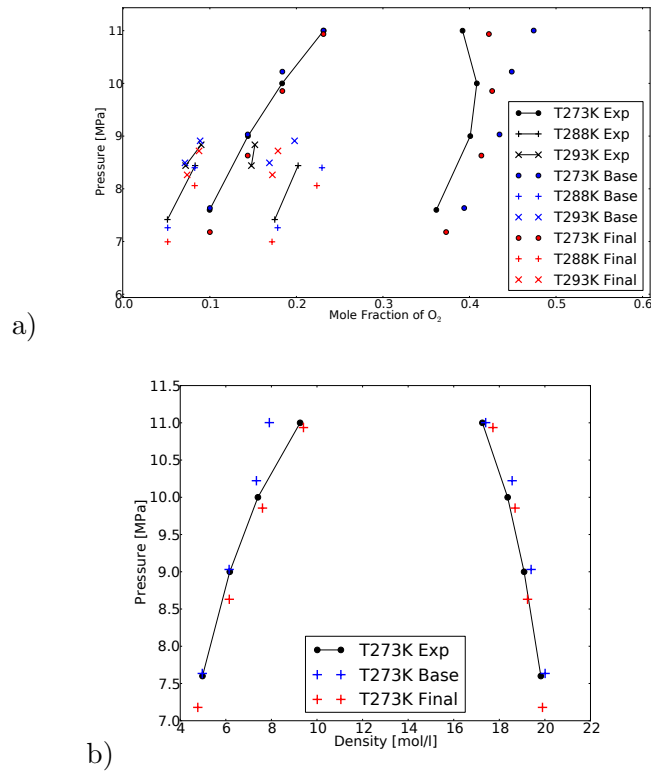


Figure 1: Comparison between measurements and simulations for coexistence properties of CO₂ + O₂ mixtures for mol fraction (a) and density (b), using literature and optimised force-fields Experimental data from Muirbrook and Prausnitz (1965) (273.15K) and Kaminishi and Toriumi (1966) (288K and 293K).

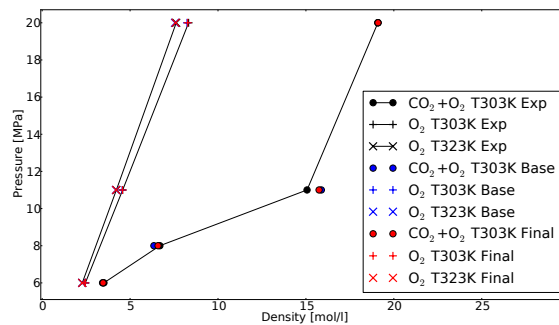


Figure 2: Comparison between CO₂+O₂ measurements and simulations for the pressure-density behaviour of the homogeneous phase, using literature and optimised force-fields Experimental data from Mantovani *et al.* (2012) (6% O₂) and Lemmon *et al.* (2011) (pure O₂).

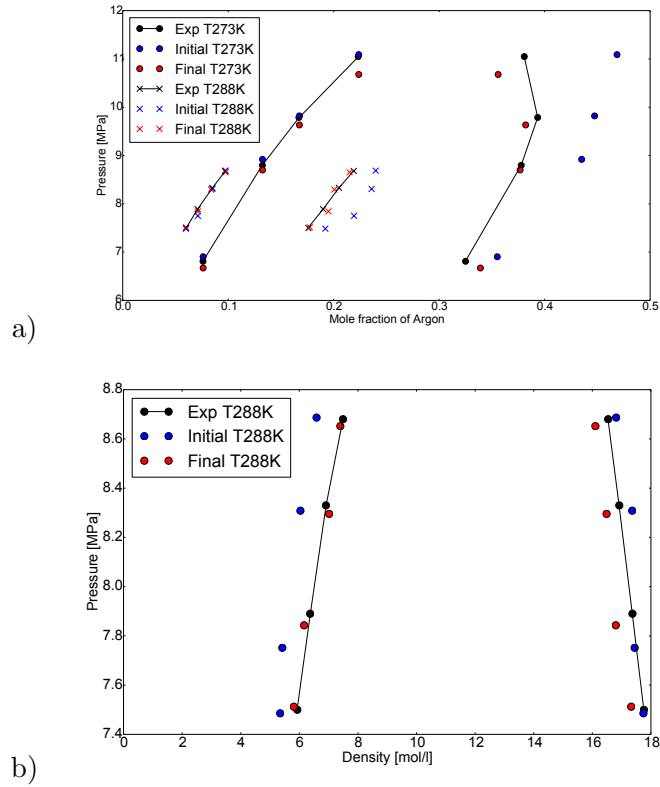


Figure 3: Comparison between measurements and simulations for coexistence properties of $\text{CO}_2 + \text{Ar}$ mixtures for mol fraction (a) and density (b), using literature and optimised force-fields Experimental data from Coquelet *et al.* (2008) and Sarashina *et al.* (1971) at 273K and 288K respectively.

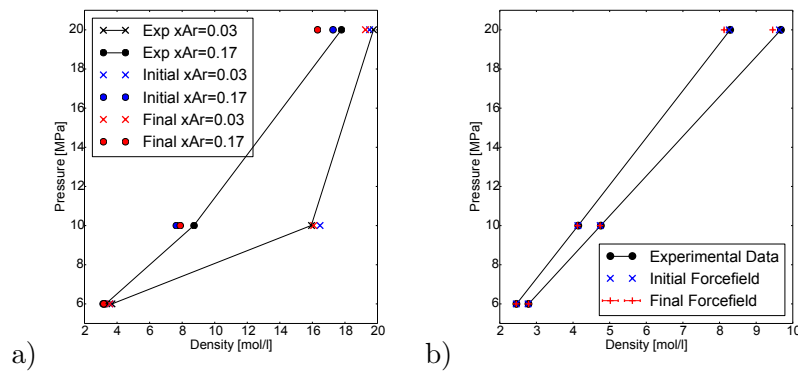


Figure 4: Comparison between $\text{CO}_2 + \text{Ar}$ measurements and simulations for the pressure-density behaviour of the homogeneous phase, using literature and optimised force-fields Experimental data from (a) Brugge *et al.* (1997) (mixtures) and (b) Lemmon *et al.* (2011) (pure Ar).

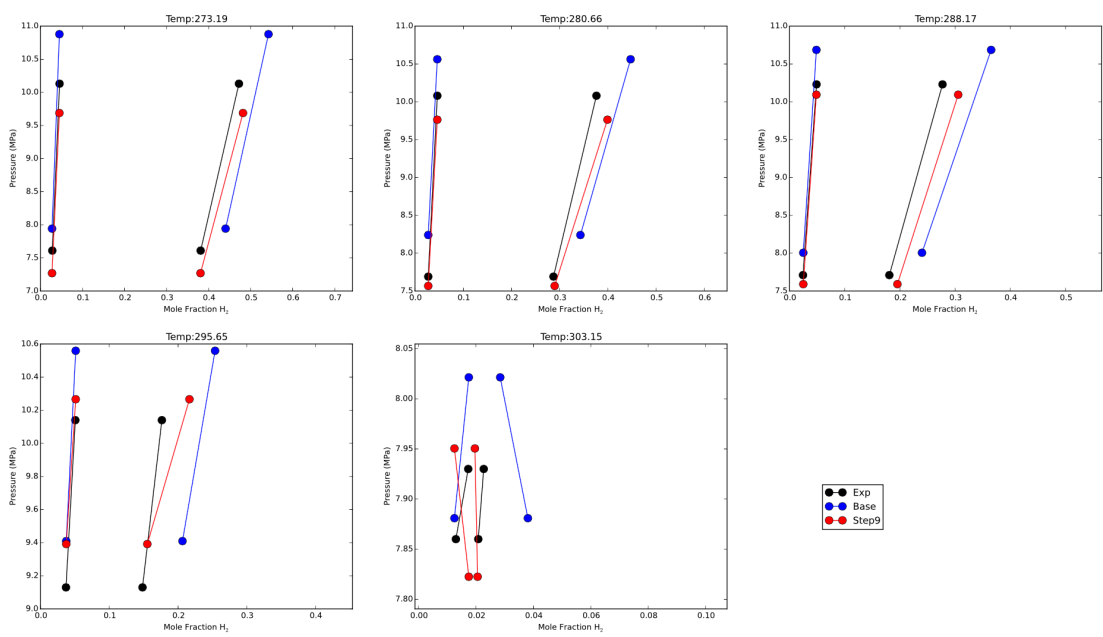
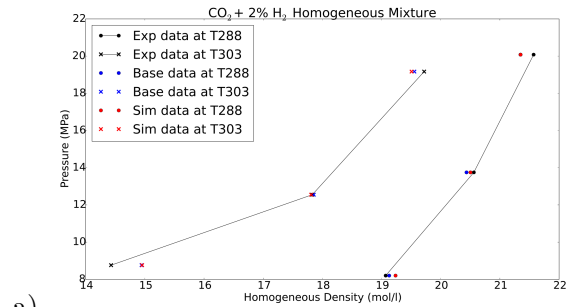
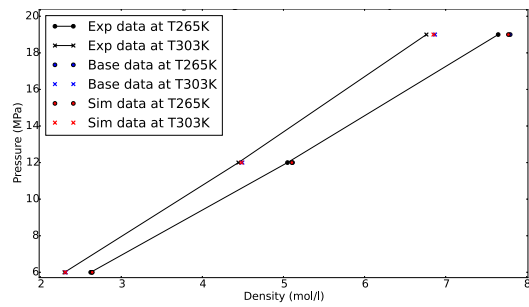


Figure 5: Comparison between measurements and simulations for the coexistence mol fraction of $\text{CO}_2 + \text{H}_2$ mixtures, using literature and optimised force-fields Experimental data from Fandiño *et al.* (2015).



a)



b)

Figure 6: Comparison between CO₂+H₂ measurements and simulations for the pressure-density behaviour of the homogeneous phase, using literature and optimised force-fields Experimental data from (a) Sanchez-Vicente *et al.* (2013) (2% H₂) and (b) Lemmon *et al.* (2011) (pure H₂).

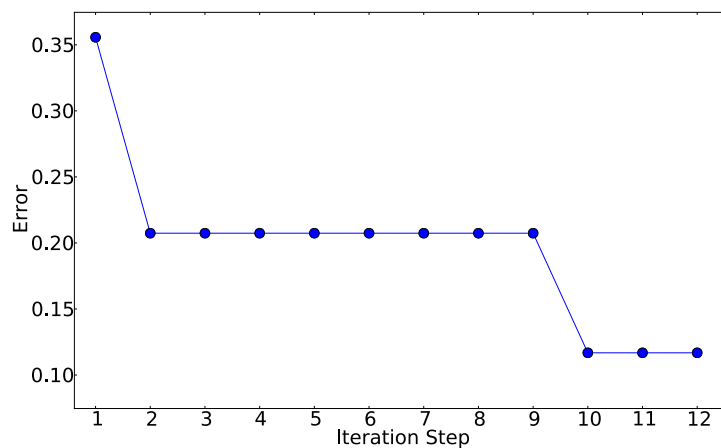


Figure 7: CO₂ + N₂ - The simplex point with the lowest error value for each iteration step after the initial simplex.

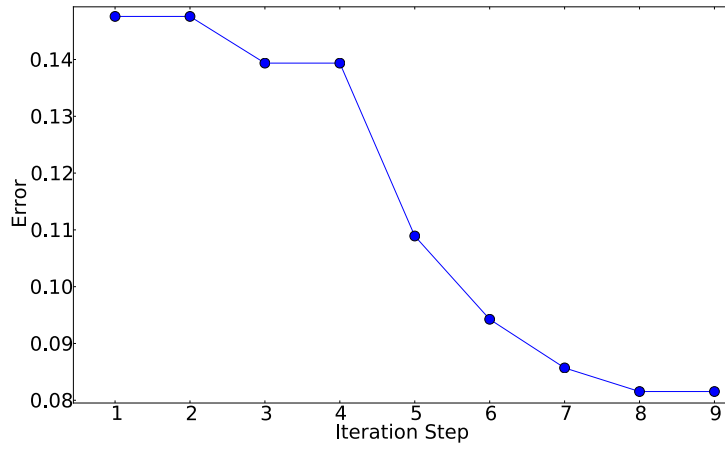


Figure 8: CO₂ + O₂ - The simplex point with the lowest error value for each iteration step after the initial simplex.

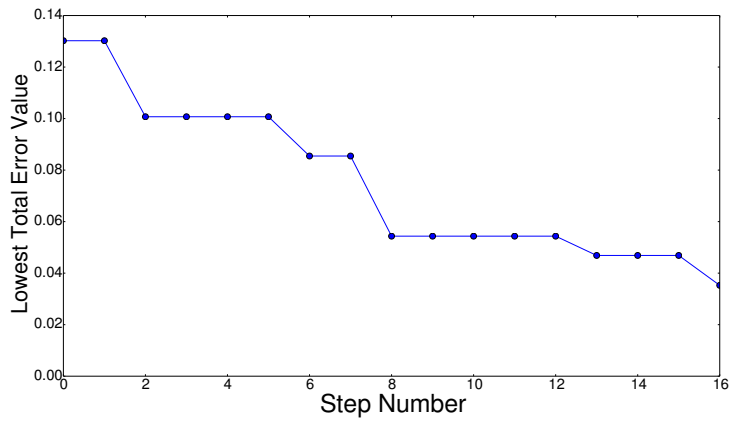


Figure 9: CO₂ + Ar - The simplex point with the lowest error value for each iteration step after the initial simplex.

2 Symmetric covariance function

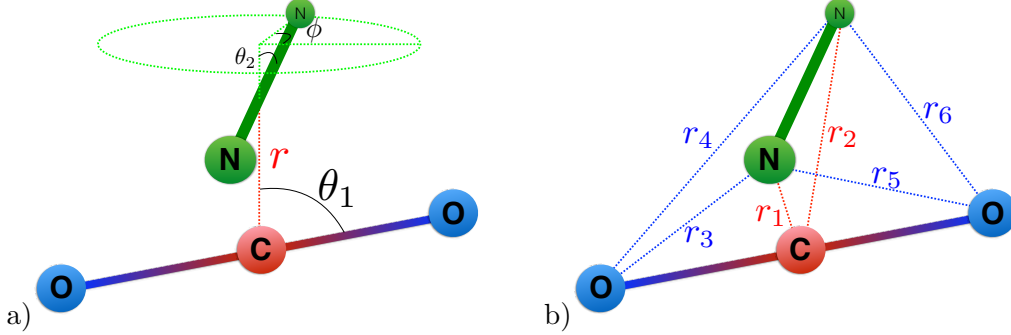


Figure 10: The geometry of a CO_2+N_2 pair, described by angles and centre of mass distance (a) and interatomic distances (b).

We used a Gaussian process (GP) to interpolate quantum-chemical calculations of the interaction between the $\text{CO}_2 + \text{N}_2$ binary pair and produce a potential energy surface, as described in the main text. We describe the $\text{CO}_2 + \text{N}_2$ binary pair via the following interatomic distances, as shown in figure 10(b): $r_1 = \text{N}^1 \rightarrow \text{C}$; $r_2 = \text{N}^2 \rightarrow \text{C}$; $r_3 = \text{N}^1 \rightarrow \text{O}^1$; $r_4 = \text{N}^2 \rightarrow \text{O}^1$; $r_5 = \text{N}^1 \rightarrow \text{O}^2$; and $r_6 = \text{N}^2 \rightarrow \text{O}^2$. We denote the inverse distances as $x_i = 1/r_i$. The intermolecular potential f between the two molecules obeys the following symmetry relations

$$\begin{aligned} f(x_1, x_2, x_3, x_4, x_5, x_6) &= f(x_2, x_1, x_4, x_3, x_6, x_5) = f(x_1, x_2, x_5, x_6, x_3, x_4) \\ &= f(x_2, x_1, x_6, x_5, x_4, x_3), \end{aligned}$$

which arise because the intermolecular potential is unchanged by flipping the N_2 molecule (so that the N_1 and N_2 atoms swap position) and, similarly for the O atoms in the CO_2 molecule. More compactly, the function

$$f(x) = f(\sigma \mathbf{x}) \forall \sigma \in K_4$$

where K_4 is the permutation group consisting of the identity permutation, e , and the following permutations (written in cyclic notation)

$$\sigma_1 = (12)(34)(56), \quad \sigma_2 = (35)(46) \quad \sigma_3 = (12)(36)(45),$$

where (12) denotes that elements 1 and 2 of x are swapped, and similarly for the additional brackets. Note that σ_1 corresponds to flipping the N_2 molecule, σ_2 corresponds to flipping the CO_2 molecule and σ_3 corresponds to flipping both molecules.

2.1 A single symmetry

To start with, suppose we want to model a function f where f is invariant under the single permutation σ , where $\sigma^2 = e$ (i.e. applying the permutation twice leaves the variables unchanged). If we assume

$$f(x) = g(x) + g(\sigma x)$$

for some arbitrary function g , then f has the required symmetry. If we model $g(\cdot) \sim GP(0, k(\cdot, \cdot))$, then the covariance function for f is

$$k_f = \text{Cov}(f(x), f(x')) = k(x, x') + k(\sigma x, x') + k(x, \sigma x') + k(\sigma x, \sigma x'),$$

If k is isotropic for each pair of variables that swap in σ (i.e. the length-scales are the same), then $k(x, x') = k(\sigma x, \sigma x')$ and $k(x, \sigma x') = k(\sigma x, x')$ as swaps only occur in pairs ($\sigma^2 = e$). So we can use

$$k_f(x, x') = k(x, x') + k(\sigma x, x'),$$

saving half the computation.

2.2 Invariance under permutations in K_4

Now consider functions that are invariant to permutations in K_4 . If we write

$$f(x) = g(x) + g(\sigma_1 x) + g(\sigma_2 x) + g(\sigma_3 x)$$

then if $g(\cdot) \sim GP(0, k(\cdot, \cdot))$

$$\begin{aligned} k_f(x, x') &= k(x, x') + k(\sigma_1 x, x') + k(\sigma_2 x, x') + k(\sigma_3 x, x') + k(x, \sigma_1 x') + k(\sigma_1 x, \sigma_1 x') \\ &\quad + \dots + k(\sigma_3 x, \sigma_3 x') \end{aligned}$$

If k is isotropic for any pair of variables that swap in any of the permutations, then $k(x, \sigma_i x') = k(\sigma_i^{-1} x, x')$. Thus $k(x, x') = k(\sigma_i x, \sigma_i x')$, $k(x, \sigma_i x') = k(\sigma_i x, x')$ and $k(\sigma_i x, \sigma_j x') = k(\sigma_k x, x')$ for $i \neq j \neq k$. Thus we can use

$$k_f(x, x') = k(x, x') + k(\sigma_1 x, x') + k(\sigma_2 x, x') + k(\sigma_3 x, x')$$

as a covariance function for f . We require that the covariance function is isotropic for any pair of inputs that swap in any of the permutations, so in the $\text{N}_2 + \text{CO}_2$ system, we require the length-scales to be the same for inputs 1 and 2 (the two C-N distances), and the same for inputs 3, 4, 5 and 6 (the four O-N distances).

References

- Brugge, H. B., J. C. Holste, K. R. Hall, B. E. Gammon and K. N. Marsh, “Densities of Carbon Dioxide + Nitrogen from 225 K to 450 K at Pressures up to 70 MPa,” *Journal of Chemical & Engineering Data* **42**, 903–907 (1997).
- Coquelet, C., A. Valtz, F. Dieu, D. Richon, P. Arpentinier and F. Lockwood, “Isothermal P, x, y data for the argon+ carbon dioxide system at six temperatures from 233.32 to 299.21 k and pressures up to 14MPa,” *Fluid Phase Equilibria* **273**, 38–43 (2008).
- Fandiño, O., J. M. Trusler and D. Vega-Maza, “Phase behavior of (CO₂+H₂) and (CO₂+N₂) at temperatures between (218.15 and 303.15)K at pressures up to 15MPa,” *International Journal of Greenhouse Gas Control* **36**, 78–92 (2015).

- Kaminishi, G. and T. Toriumi, "Gas-liquid equilibrium under high-pressure VI. Vapor-liquid-phase equilibrium in the CO₂-H₂, CO₂-N₂ and CO₂-O₂ systems." *Kogyo Kagaku Zasshi* **69**, 175-178 (1966).
- Lemmon, E., M. McLinden and D. Friend, "Thermophysical Properties of Fluid Systems in NIST Chemistry WebBook, NIST Standard Reference Database Number 69, Eds. P.J. Linstrom and W.G. Mallard, National Institute of Standards and Technology, Gaithersburg MD, 20899," (2011).
- Mantovani, M., P. Chiesa, G. Valenti, M. Gatti and S. Consonni, "Supercritical pressure-density-temperature measurements on CO₂-N₂, CO₂-O₂ and CO₂-Ar binary mixtures," *The Journal of Supercritical Fluids* **61**, 34-43 (2012).
- Muirbrook, N. and J. Prausnitz, "Multicomponent vapor-liquid equilibria at high pressures: Part I. Experimental study of the nitrogen-oxygen-carbon dioxide system at 0C," *AIChE Journal* **11**, 1092-1096 (1965).
- Sanchez-Vicente, Y., T. C. Drage, M. Poliakoff, J. Ke and M. W. George, "Densities of the carbon dioxide + hydrogen, a system of relevance to carbon capture and storage," *International Journal of Greenhouse Gas Control* **13**, 78-86 (2013).
- Sarashina, E., Y. Arai and S. Sasto, "The P-V-T-X relation for the carbon dioxide-argon system," *Journal of Chemical Engineering of Japan* **4**, 379-381 (1971).